Bio-Design and Manufacturing (2026) 9:100–121
https://doi.org/10.1631/bdm.2500027

REVIEW

# Tissue engineering tubular scaffold fabrication for esophageal regeneration

Xingyu Zhou[1] · Xianglin Zhang[1] · Bin Wu[1]

Received: 21 January 2025 / Accepted: 14 June 2025
© Zhejiang University Press 2026

## Abstract

The esophagus is a tubular organ essential for maintaining normal eating function in humans. However, the replacement of the esophagus remains challenging in clinical settings. Although tissue engineering scaffolds are a promising alternative solution, their fabrication is difficult due to the complex structure and function of the esophagus. This review describes the existing fabrication methods for esophageal tubular scaffolds, including decellularization, casting, electrospinning, three-dimensional (3D) bioprinting, and pin-frogging. Also discussed are the stimulation cues of the fabricated esophageal tubular scaffold that induce esophageal muscle and epithelial cells. Finally, this review emphasizes three important concerns for esophageal tubular scaffolds: leakage and porosity, elasticity and proliferation of smooth muscle cells, and biocompatibility and structural fidelity of biomaterials.

## Graphical abstract

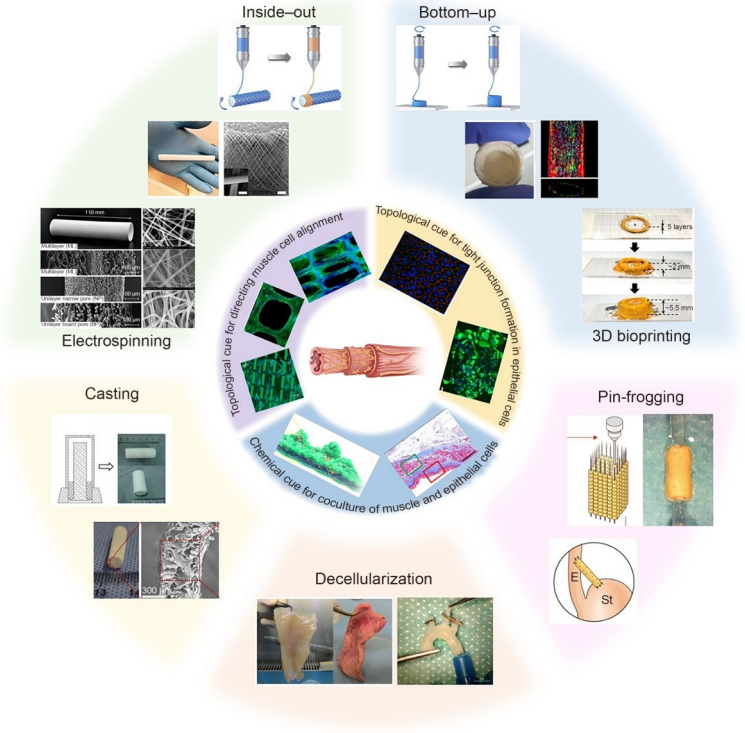


**Keywords** Esophageal tissue engineering · Decellularization · Casting · Electrospinning · Three-dimensional (3D) bioprinting

✉ Bin Wu
wubin19@hust.edu.cn

[1] State Key Laboratory of Materials Processing and Die & Mould Technology, School of Materials Science and Engineering, Huazhong University of Science and Technology, Wuhan 430074, China

## 1 Introduction

The esophagus is a part of the digestive tract that connects the throat to the stomach. Its primary function is to provide a channel and necessary force for transporting food during swallowing, thus playing a vital role in maintaining human health and well-being. Nevertheless, if the esophagus is injured due to trauma or cancer [1], the swallowing process gets interrupted, causing difficulties in eating and even death. Gastric lifting surgery is the gold standard for repairing an esophageal defect [2]. Autografts such as the colon, jejunum, and other gastrointestinal tracts can also be used to replace a damaged esophagus. However, the structures of the gastrointestinal tract differ from those of the esophagus and cannot entirely mimic esophageal function. Hence, these autografts typically result in severe, difficult-to-treat complications, such as esophageal stenosis, fistula, and leakage. Consequently, the five-year relative survival rate of patients with esophageal cancer is only 22%, ranking penultimate among the rates of all cancer types [3]. Therefore, it is necessary to develop new methods for constructing artificial bionic esophagi and improving patient survival rates.

Previous studies have demonstrated the potential of tissue engineering methods for addressing the challenges of esophageal defects [4–9]. These methods involve the use of biomaterials to prepare scaffolds that are then combined with cells to repair esophageal defects and restore esophageal function. An ideal biomimetic esophageal scaffold should provide good biocompatibility, mechanical strength, and suitable stimulation cues, such as topology, stiffness, and chemical signals, to induce cells to form functional tissues. This review discusses the current fabrication methods (Table 1) along with their limitations and future development trends in esophageal tissue engineering (ETE), thereby providing assistance for the future development of esophageal tubular scaffolds.

## 2 Structural analysis and design of the esophagus

While designing and fabricating a perfect artificial esophageal scaffold, we first analyze the structure and function of the natural esophagus. The primary structure of the natural esophagus consists of mucosal and muscle layers. The mucosal layer acts as a barrier for the entire esophagus and comprises a dense layer of squamous epithelial cells (SECs), which collectively reduce the friction and mechanical stress caused by the movement of food [10]. The muscle layer is located outside the mucosal layer and comprises two sublayers of muscle fibers that are perpendicular to each other, i.e., the inner annular layer and outer longitudinal layer. These layers are primarily composed of smooth muscle cells (SMCs) and skeletal muscle cells. The impetus for the food movement originates from the alternating contraction of these two layers of muscle fibers. Therefore, an ideal artificial esophageal scaffold should have a double-layer structure that mimics the mucosal and muscle layers. Internally, the mucosal layer should be a flat membrane that allows SECs to grow and differentiate evenly and densely. Externally, the muscle layer should include an inner annular and outer longitudinal structure, guiding the directional growth of SMCs.

To achieve a uniform direction for muscle cells, structural features that provide directional guidance for the growth of muscle bundles and create a favorable microenvironment for tissue growth are essential. It is also important to consider the paracrine role between muscle cells and SECs to coordinate the co-growth of multiple layers of esophageal cells. Furthermore, the esophageal tubular scaffold must possess sufficient mechanical properties for suturing the digestive tract [11]. Challenges concerning material selection, manufacturing methods, and cell induction must also be considered while designing and fabricating an esophageal tubular scaffold.

The design of bionic esophageal scaffolds can be traced back to 1952, when Berman from the United States first designed and prepared a round tubular polyethylene artificial esophagus [12]. Today, tissue engineering for esophageal replacement is a rapidly growing area of research, and numerous methods have been developed for preparing artificial esophagi that meet the required specifications. As mentioned earlier, the key point of artificial esophageal scaffold printing is that the multilayer structure and the difference in the inner and outer layer structures guide the growth of different cells. In recent years, several new methods have been developed for ETE. This review discusses the current ETE fabrication methods, including (i) decellularization [13–17], (ii) casting [18–24], (iii) electrospinning [4–6, 25–35], and (iv) three-dimensional (3D) bioprinting [7, 8, 36–40]. Moreover, this review cites a case of a scaffold prepared by combining electrospinning and 3D bioprinting using a novel "pin-frogging" method for esophageal scaffold preparation [41] (Fig. 1).

## 3 Decellularization of the animal esophagus

Natural esophagus decellularization differs from allograft donation as it involves the eradication of live cells and genes of the original tissue. The decellularized tissue still contains various residual proteins, which are favorable for cell growth. ETE is a promising approach for creating esophageal alternatives, and various non-degradable and

**Table 1** Summary of esophageal scaffolds prepared using various processes

| Preparation process | Main material | Structure | Porosity (%) | Mechanical parameters (MPa) (Young's modulus: $E$; maximum tensile strength: $\sigma$) | In vitro test results | In vivo test results | Ref. |
|---|---|---|---|---|---|---|---|
| – | Natural esophagus | Three layers | – | $E$: 2.30 (longitudinal); 1.44 (radial) $\sigma$: 2.19 (longitudinal); 1.41 (radial) | – | – | [11] |
| Decellularization | Porcine esophagus | – | – | – | – | Muscle tissue regenerates around the esophagus, and the average body weight increases | [16] |
| | Porcine small intestinal submucosa | – | – | – | – | Development of the muscle layer and immature epithelial cells | [42] |
| | Rat esophagus | – | – | – | Smooth muscle cells differentiate into a bilayer structure that resembles the natural esophagus, with the formation of new blood vessels | – | [14] |
| Casting | Silk fibroin (SF) | Double layer | – | $E$: 1.7±0.16 $\sigma$: 0.29±0.04 | – | There was significant host tissue growth at the original graft site, and the lumen cross-sectional area of the repaired catheter significantly increased by 4.5-fold | [22] |
| | Polyester urethane (PU)+SF | The SF surface is grafted onto a PU bracket | – | – | – | The scaffold promotes the growth of smooth muscle after injury, giving it a normal inner and outer longitudinal bilayer musculature | [21] |
| | Poly(L-lactide-co-caprolactone) | Inner cylinder+ outer tube composed of silicone stopper | – | $\sigma$: 1.78±0.57 | Improved cell viability | After 5–6 months of implantation in the pig's esophagus, there is a near-intact layer of epithelial cell regeneration around the lumen when the scaffold is degraded | [20] |
| | Crosslinked poly(ester urethane) (CPU)+ SF | Double layer: CPU-SF channel+ decellularized esophageal mucosa | – | – | Biomimetic scaffolds can guide cell growth | – | [23] |

To be continued

Table 1 (continued)

| Preparation process | Main material | Structure | Porosity (%) | Mechanical parameters (MPa) (Young's modulus: $E$; maximum tensile strength: $\sigma$) | In vitro test results | In vivo test results | Ref. |
|---|---|---|---|---|---|---|---|
| Electrospinning | Nylon 6/SF+ collagen (COL)/ chitosan (CS) | Nylon 6/SF nanofiber pads+ COL/CS modification | 75±1.4 | $\sigma$: 13.80±0.20 | Excellent cytophilicity that promotes cell adhesion and proliferation | New blood vessel formation, which facilitates the healing of esophageal defects | [4] |
| | Poly-L-lactide-copoly-ε-caprolactone | Cylindrical/ asymmetrical | – | $E$: 0.97±0.10 (cylindrical); 0.39±0.07 (asymmetrical) $\sigma$: 6.09±0.21 (cylindrical); 6.22±0.01 (asymmetrical) | After 14 d of incubation, cell proliferation significantly increased in both scaffolds, with the asymmetric scaffolds exhibiting higher cell viability | At the end of the 7-d follow-up, all four animals were alive | [35] |
| | Polyamide-6 | – | 90 | $E$: 202.3±12.5 (dry); 39.5±3.6 (wet) $\sigma$: 23.8±1.1 (dry); 18±0.8 (wet) | It has good cytocompatibility | – | [5] |
| | Polyurethane | – | 78±1.1 | $E$: approximately 2.5 $\sigma$: approximately 6 | Releases angiogenesis and immunomodulatory proteins | Reconstructs the mucosa, submucosa, and muscularis of the esophagus, which is histologically similar to the natural, intact esophagus | [31] |
| | Polycarbonate-based polyurethane polymers | Three layers: sparse on the outside and dense on the inside | – | – | Different cell growth is supported in different layers, with a small pore layer in the middle separating the two cell populations | – | [6] |
| | Poly(3-hydroxybutyrate-co-3-hydroxyvalerate)+ gelatin | – | 97.6±0.3 | $E$: 236.19±26.37 $\sigma$: 2.37±0.18 | Supports esophageal regeneration, has good cytocompatibility, and is degradable | – | [25] |
| | Polyethylene oxide+PU | Double layer | – | – | Simultaneous differentiation of stem cells into desired cell lineages | – | [33] |
| | Polycaprolactone (PCL) | Monolayer | – | $E$: 13.5±0.7 $\sigma$: 1.6±0.5 | After evaluating cell morphology, mitochondrial activity, immunohistochemistry, and western blotting results, the coated PCL/SF scaffold was confirmed to be optimal for the proliferation and differentiation of porcine primary epithelial cells | Using a PU scaffold as a physical support, an in situ implantation test demonstrated that the coated PCL/SF had good biocompatibility and ability to promote the regeneration of defective epithelium | [34] |
| | PCL/SF | | – | $E$: 11.6±1.0 $\sigma$: 1.9±0.3 | | | |
| | SF | | – | $E$: 37.2±0.8 $\sigma$: 2.9±0.9 | | | |

To be continued

Table 1 (continued)

| Preparation process | Main material | Structure | Porosity (%) | Mechanical parameters (MPa) (Young's modulus: $E$; maximum tensile strength: $\sigma$) | In vitro test results | In vivo test results | Ref. |
|---|---|---|---|---|---|---|---|
| | Poly(D,L-lactic-co-glycolic acid) (PLGA) | – | – | – | The cells are dense and proliferating, with little to no apoptosis | The vascular-like structure is clearly delineated | [27] |
| | PLGA/PCL | – | – | – | As the PCL concentration increases, the level of proliferation and cell density decrease | The vascular-like structure is clearly delineated, and the number of blood vessels is large | |
| | PU | – | 86.25±0.87 | – | The mucosal cells attach well to the surface of the PU graft and form multiple layers | Full-thickness tissue regeneration occurred in the graft area of the esophagus, and several blood vessels formed within the newly formed tissue | [29] |
| | Polydioxanone | – | 87.20±0.80 | – | Cells attached initially but began to degrade on Day 5 | – | |
| | Poly(L-lactide-co-ε-caprolactone) | – | – | – | Cells attached and proliferated well on the scaffold. After 90 d of seeding cells on the scaffold, >6% cell viability was observed | – | [28] |
| | PCL+paclitaxel | – | 68.4–73.7 | – | A higher inhibition rate of SMC proliferation was observed in vitro on fibrous membranes with higher paclitaxel content, and tissue inflammation and collagen fiber proliferation were significantly reduced | – | |
| | Small intestine submucosa/PLGA | – | 83–91 | – | The cells are arranged along the fibers and have a high level of biocompatibility | The inflammatory response is triggered by cellular infiltration and encapsulation | [32] |
| 3D printing | Methylcellulose+polycaprolactone+poly[(caprolactone)–glycolide copolymer]+polyethylene glycol+glycerol | Monolayer | – | $E$: 37.3<br>$\sigma$: 2.18 | Does not elicit an immunogenic response, and epithelial cells can easily colonize and proliferate on the printed scaffold | – | [7] |

To be continued

Table 1 (continued)

| Preparation process | Main material | Structure | Porosity (%) | Mechanical parameters (MPa) (Young's modulus: $E$; maximum tensile strength: $\sigma$) | In vitro test results | In vivo test results | Ref. |
|---|---|---|---|---|---|---|---|
| | Resin+ decellularized extracellular matrix (dECM) | Single-layer tubular (smooth on the inside/ rough on the outside) | – | – | Provides a suitable microenvironment for promoting cellular activity; Transdifferentiation of fibroblasts into myofibroblasts | – | [38] |
| | Thermoplastic polyurethane/ poly(lactic acid) | Single-layer spiral scaffold | – | – | Human esophageal epithelial cells grow and proliferate on scaffolds, indicating that the scaffold after the printing process is biocompatible | – | [37] |
| | Medical-grade PCL+dECM | Multilayer free-form tubular structure+filled with bioink | – | $\sigma$: 7.15±1.3 | It has a porous multilayer structure that promotes cell proliferation, thereby improving cell proliferation and viability | – | [8] |
| 3D printing+ electrospinning | PCL | PCL reinforcing ring+ electrospun fiber layer | – | – | Not cytotoxic | The artificial periesophageal defect heals completely, and as the infiltrated host cells enter the scaffold, the structural integrity is maintained, with only a slight inflammatory response and minimal granulation tissue; Squamous epithelial cells and soft tissue regeneration | [43] |
| | PU+PCL | Double layer | – | $\sigma$: 4.5 | Most cells were well distributed on the nanofiber structure, and the proliferation of cells on the nanofiber structure increased over time | The esophageal scaffold is intact in its integration with its natural esophageal tissue and is covered with a multilayered squamous epithelium and several newly developed blood vessels | [9] |
| Pin-frogging | Normal human dermal fibroblasts+ human umbilical vein endothelial cells+ mesenchymal stem cells | Monolayer | – | – | Produces elastin and microvasculature | Epithelialization of the surface of the structural lumen occurs. In the outer epithelial layer, smooth muscle cells are maintained and muscle fibers are distinct | [44] |

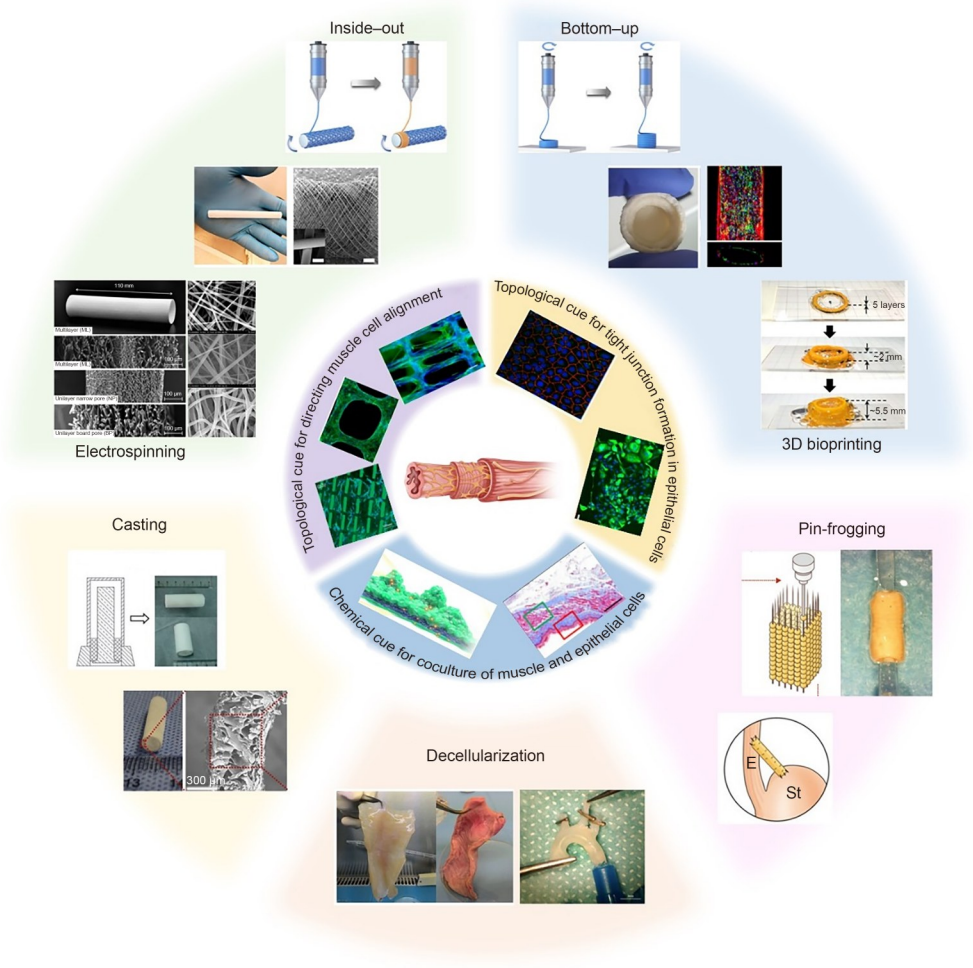


**Fig. 1** Different fabrication methods for the preparation of esophageal tubular scaffolds

biodegradable esophageal scaffolds have been developed to date. For instance, Luc et al. [45] investigated nonabsorbable, polymer-resorbable, and decellularized matrix scaffolds for esophageal repair. The removal of nonabsorbable scaffolds post-surgery may result in esophageal strictures, and tissue regeneration is insufficient in the presence of larger defects. Polymer-resorbable scaffolds may release toxic degradation products at an uncontrolled rate, resulting in structures that differ from native tissues. In contrast, acellular matrix tubes have advantages that are similar to those of native tissues and support cell proliferation [45]. In recent years, biological scaffolds composed of acellular tissue-derived extracellular matrices (ECMs) have been increasingly used in regenerative medicine [2, 46–52]. For instance, Beckstead et al. [53] demonstrated that the decellularized human dermis provided a more favorable structure for epithelial tissue than cell-seeded polymer scaffolds. Decellularized matrices contain the same components as ECMs, such as glycoproteins, proteins, glycosaminoglycans, and proteoglycans. These matrices can mimic the biological and mechanical functions of native ECMs and possess a 3D structure with a microenvironment conducive to cell proliferation and directed growth [54].

The key to the process of decellularization is removing cells from the natural esophagus [55]. After decellularization, the remaining matrix contains the native cytoplasmic matrix but no cellular or genetic material, thereby preventing postimplantation immune rejection. The decellularized stromal tube depicted in Fig. 2a appears translucent compared with the native esophagus due to the removal of cells and their contents [16]. To increase the contact area of the decellularized matrix tube, it can either be combined with a polymer scaffold or perforated. For instance, Marzaro et al. [16] developed a valuable homologous decellularized esophageal scaffold for use in esophageal replacement methods. They perforated the scaffold such that it had a porous network (Fig. 2b), allowing cells to effectively colonize the outer and inner surfaces of the scaffold without damaging its size or structure. After implantation of the scaffold into a large animal model, the observed regeneration of the muscle demonstrated good cytocompatibility of the scaffold and its ability to promote cell proliferation (Fig. 2c).

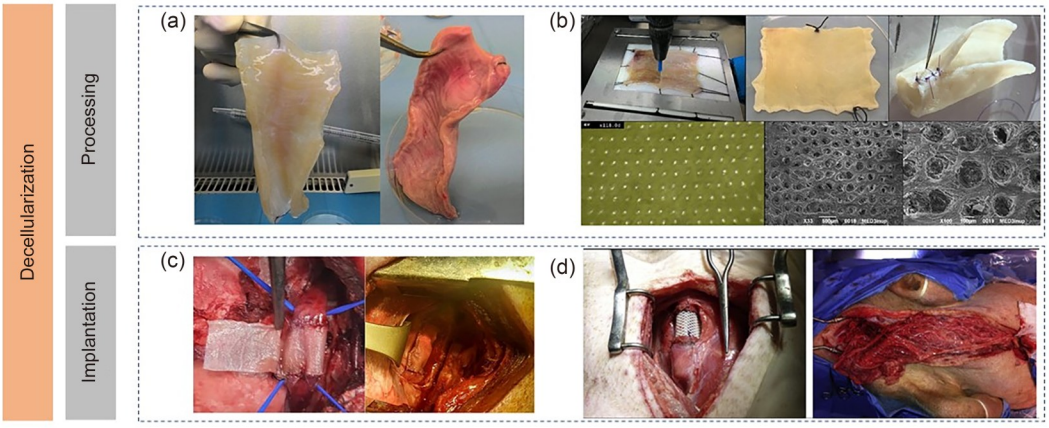


**Fig. 2** Esophageal tissue engineering scaffold prepared using the decellularization method. (a) Decellularized esophagus (left) versus natural esophagus (right). (b) Appearance and scanning electron microscope (SEM) images of the decellularized matrix tube after perforation. (c) Surgical implantation of acellular stromal tubes. Reproduced from [16], licensed under CC BY-NC 4.0. (d) Implantation of an artificial esophageal scaffold after esophagectomy. Reproduced from [42], with permission from Elsevier Inc.

Furthermore, Poghosyan et al. [42] used a decellularized stromal tube rather than an artificial esophagus. They performed circumferential excision of the porcine esophagus and sutured the artificial esophageal substitute (Fig. 2d). The esophagus was found to function normally in only a few weeks; however, after a month or more, the pigs used in the experiments presented different degrees of inflammation or esophageal stricture. Therefore, the long-term in vivo adaptability of the scaffold still requires improvement.

Although decellularized matrix scaffolds provide a favorable microenvironment for cell growth and proliferation, they pose certain challenges, including an insufficient pore density for large numbers of cells to attach and a lower mechanical strength than polymer scaffolds. Several methods combining acellular matrices with cast or 3D-printed scaffolds have been developed to achieve the complex structure and excellent biological and mechanical properties of the natural esophagus.

## 4 Casting of esophageal tissue engineering tubular scaffolds

Casting is the easiest and most commonly used process for preparing various types of tissue engineering scaffolds. A scaffold structure with an ideal wall thickness and pore size can be conveniently prepared by designing a casting mold. Ordinary casting can only produce smooth, round tubes and cannot replicate the complex structure of the esophagus; hence, it is essential to combine methods to improve the morphological characteristics of the obtained round tubes. To visualize the multilayer structure of the esophagus and the directional arrangement of muscle bundles in the muscle layer, thermally induced phase separation (TIPS) has been used to construct two-layer scaffolds with varying pore sizes. This approach improved the mold structure, and microgrooves were cast on the scaffold surface to induce directional cell growth.

As depicted in Fig. 3a, the mold used to prepare this scaffold consisted of two components, i.e., an inner cylinder and an outer tube, which were connected via silicone plugs. The gap between these two components determines the wall thickness and pipe diameter of the obtained bracket [20]. The poly(L-lactide-co-caprolactone) (PLLC) solution was slowly injected into the voids of the mold before quenching to 23 °C for 1 h to induce the coarsening effect and freeze-drying to obtain a double-layer artificial esophageal substitute. Hou et al. [20] established a method for designing porous scaffolds using TIPS. By carefully selecting process parameters such as solvent type, polymer concentration, and roughening conditions, the pore size can be adjusted within the range of 10–200 mm. An increase in coarsening time typically results in pore enlargement [56], which is caused by the differential interfacial tension applied between the two-phase separation domains composed of polymer-rich phase and polymer-lean phase. The duration of the coarsening process is related to the porosity, pore size distribution, and interconnectivity of the resulting scaffold. When the roughening process is prolonged, the pore connectivity and porosity decrease, and the scaffold may even collapse owing to the coalescence of the sparse domains of the polymer and the gravitational pull of the polymer itself [57].

Figure 3a depicts the microstructure of the prepared scaffold, wherein all bulk structures are highly porous and interconnected. Considering the structure of the natural esophagus, a main feature of the tubular scaffold is its asymmetrical pore size distribution, with an area of 10–50 $mm^2$ around the lumen and 20–200 $mm^2$ for most of the tube wall. This asymmetrical structure facilitated the maintenance of the initial mechanical strength of the scaffold and

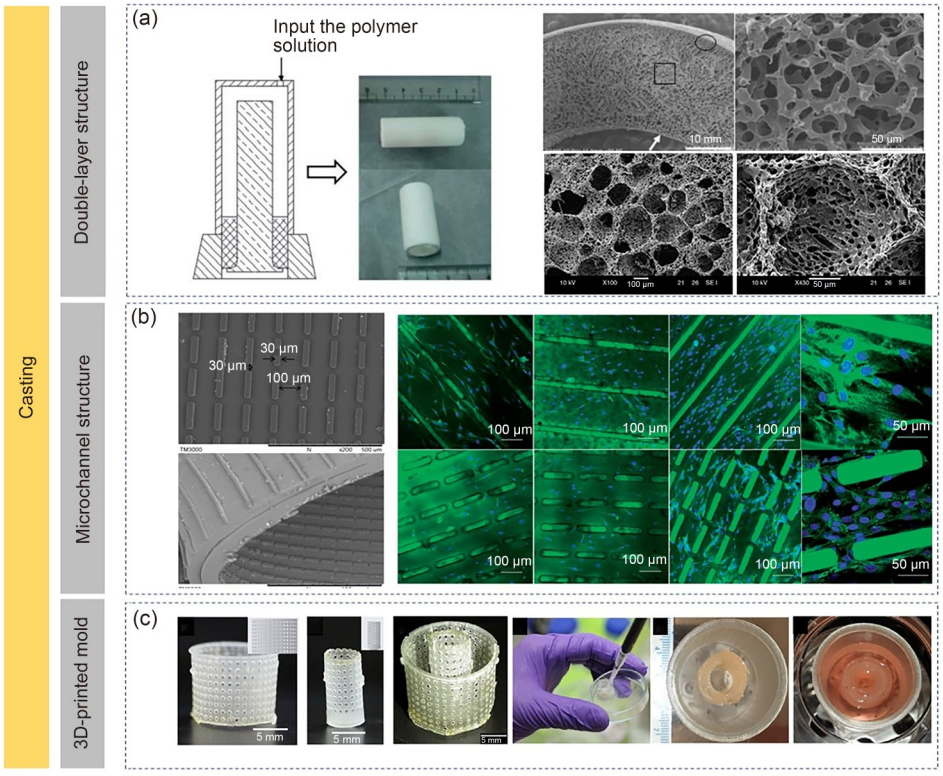


**Fig. 3** Esophageal tissue engineering scaffold prepared using the casting method. (a) Considering the natural esophageal structure, a double-layer structure with different porosities was prepared. Reproduced from [18] (with permission from Elsevier B.V.) and [20] (licensed under CC BY 4.0). (b) Artificial esophagus with a special microchannel structure designed to induce the orientation of esophageal myocytes. Reproduced from [21], licensed under CC BY 4.0. (c) A polymer scaffold is used as a mold to fill with bioink. Reproduced from [38], with permission from the American Chemical Society

supported tissue regeneration through efficient mass transfer [20]. In vitro cell culture and animal implantation experiments confirmed that the scaffold significantly improved the cells' survival rate. When the scaffold was degraded, a layer of almost intact SECs regenerated around the lumen, demonstrating good biocompatibility of the scaffold.

However, as mentioned earlier, the primary structure of the natural esophagus includes the mucosal and muscle layers. Promoting the production of SMCs and controlling the direction of muscle cell growth are essential for artificial esophageal replacement. Therefore, Hou et al. [21] used solution casting to prepare a polyester urethane (PU) scaffold and then grafted glutaraldehyde and silk fibroin (SF) to its surface. In addition, the scaffold surface was coated with vascular endothelial growth factor, thereby improving the biocompatibility of the scaffold and promoting the in vivo regeneration of blood vessels. The 3D microgroove scaffold depicted in Fig. 3b was designed according to the typical structure of the esophageal muscle tissue, with the lateral groove guiding longitudinal muscle cells and the inner groove guiding annular muscle cells. The discontinuous groove wall facilitated the penetration of cells into the groove ring through a loop. α-Smooth muscle actin (α-SMA), the major isoform of actin in SMCs, exhibits high sensitivity and specificity for SMCs and is often used to detect their location and activity. The expression of α-SMA (green fluorescence) on the scaffold increased gradually over time between cultures (Fig. 3b), indicating the growth of cells on the scaffold. The longer the culture, the greater the number of cells that survived. As the number of cells increased, the morphology of the cells arranged along the microgrooves became more pronounced, and a few cells even communicated with other cells through the extension of slits. Subsequent in vivo experiments demonstrated that the scaffold promoted the growth of SMCs after injury, resulting in a standard inner ring and outer longitudinal bilayer muscle structure. If the scaffold is combined with the electrospinning basement membrane and decellularized submucosa, the entire esophagus can be constructed.

Similarly, Seth et al. [19] and Algarrahi et al. [22] used solvent casting/salt leaching to prepare a bilayer SF scaffold with mechanical properties similar to those of the native esophagus. They detected significant host tissue growth at the graft site after in vivo transplantation and a significant increase (4.5-fold) in the lumen cross-sectional area of the

repaired diseased catheter. Furthermore, crosslinked PU/SF scaffolds prepared by combining the casting method with acellular esophageal mucosa provided sufficient growth space to guide cell growth and improve the cell survival rate [23].

As shown in Fig. 3c, Yeleswarapu et al. [38] used the stereolithography apparatus technology to print two concentric resin cylinders, which were then combined and filled with a cell-encapsulated decellularized ECM (dECM) hydrogel. Integrating the polymer framework with the acellular matrix improved the mechanical properties and structural appearance of the dECM hydrogel and also retained the functionality of the acellular matrix.

To summarize, casting is a feasible method for fabricating artificial esophageal substitutes with good biocompatibility, adjustable wall thickness, and scaffold porosity, which can be achieved by controlling the mold shape, post-treatment methods such as roughening, and the addition of suitable additives. Nevertheless, a limitation of this process is that it provides negligible flexibility in shape and size. Most scaffolds prepared using the casting method exhibit large pores (400 μm to 200 mm) [19, 20, 22] and no fixed pore size, dramatically reducing the area in which cells can be attached and grown. Furthermore, this process lacks precise control over mechanical strength, and the ultimate strength of its scaffolds (0.29–1.78 MPa) is lower than that of scaffolds prepared through electrospinning or 3D printing (1.6–23.8 MPa). This means that the scaffold prepared by the casting method cannot play a proper supporting role due to the lack of mechanical strength. The function of a scaffold prepared using casting is influenced by the random distribution of cellular components, which does not reflect the complex structure of the natural esophagus. Therefore, the casting method is limited and not ideal for preparing artificial esophageal scaffolds.

## 5 3D printing techniques for esophageal tissue engineering tubular scaffolds

3D printing technology is a relatively new ETE method that enables the creation of products with an ideal structure by controlling the path movement and diameter of the nozzle. Based on the requirements of the multilayer structure of the esophagus and the morphology of its different layers, we categorized the existing 3D printing methods for ETE scaffolds into two printing strategies, i.e., the "inside–out" and "bottom–up" strategies.

### 5.1 Electrospinning of an esophageal tube based on the "inside–out" strategy

Formhals investigated the electrospinning mechanism in the 1930s [58, 59]. An electrospinning process typically involves the following three key components: a high-voltage power source, a spinneret, and a collector. A high voltage is applied between the spinneret and collector, and a solution is then extruded through the nozzle, which becomes charged under the influence of the electric field. The initially straight jet experiences intense agitation or splitting as a result of bending instability, leading to further elongation. Ultimately, the fibers solidify and are deposited onto the collector [60].

In a high-voltage electric field, the liquid extruded from the spinneret becomes charged. Moreover, it forms a continuous conical jet when the forces of the electric field, gravity, surface tension, and viscous stress reach equilibrium. This cone is referred to as the "Taylor cone." Moreover, factors such as electrode configuration and applied electric potential affect the behavior of the extruded liquid [61]. To facilitate research, liquid and gas can be considered incompressible, viscous, and nonrotating phases, and the conservation of mass for the entire region can be expressed as Eq. (1) [62]:

$$\nabla \cdot \vec{V} = 0, \tag{1}$$

where $\vec{V}$ is the velocity vector.

Introducing surface tension at the liquid–gas interface ($\vec{F}_S$), electrical force ($\vec{F}_E$), and gravitational force, the Navier–Stokes equation can be expressed as Eq. (2) [62]:

$$\rho \frac{d\vec{V}}{dt} = -\nabla P + \mu \nabla^2 \vec{V} + \rho \vec{g} + \vec{F}_S + \vec{F}_E. \tag{2}$$

The properties of the liquid and the applied voltage are important control parameters to generate the desired jet and droplet size, a principle that also applies to electrospinning.

There are two major electrospinning strategies to prepare an artificial esophageal tubular scaffold. The first strategy involves initially printing a flat film via electrospinning [30, 63, 64] and then bending and folding the film to form a cylindrical 3D fiber structure. The advantage of this strategy is that the equipment can be operated in a relatively simple manner; however, there may be stress concentration at the contacted seam. The second strategy involves direct spinning of raw materials for the scaffold onto a cylindrical collector, followed by peeling off the hollow cylindrical structure [6, 9, 33, 34]. This method requires the matching of the relative movements of the spinneret and cylindrical collector. Although the equipment is cumbersome to operate and control, it does not exhibit stress concentration.

As illustrated in Fig. 4a, electrodynamic jetting (E-jetting) can generate regular mosaic structures on the collector with high spatial accuracy and 3D resolution. E-jetting, also known as near-field electrospinning, is a specialized electrospinning technique. The technology works similarly to electrospinning, using a high-voltage electric field to electrify the droplets, and the electric field force drives the droplets

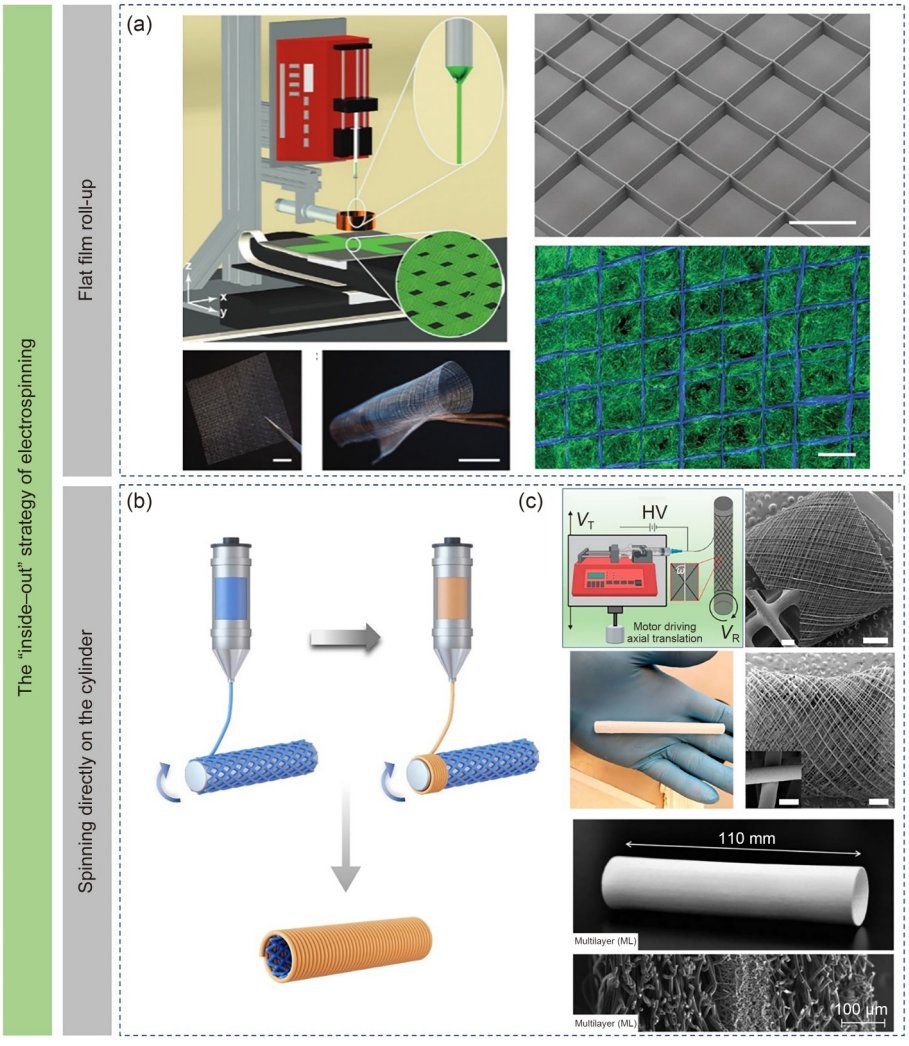


**Fig. 4** The "inside–out" strategy of electrospinning to create artificial esophageal scaffolds. (a) First, electrospinning is used to print a flat film, and then the film is rolled up to form a tubular structure. Reproduced from [30], with permission from WILEY-VCH Verlag GmbH & Co. KGaA, Weinheim. (b) Schematic of the "inside–out" strategy. (c) Direct spinning on the cylinder: the advantage is that there is no problem of stress concentration, and the disadvantage is that the two devices need to match the movement. The regulation is more complicated. Reproduced from [6] (with permission from Wiley Periodicals, Inc.) and [34] (with permission from the American Chemical Society)

to produce extremely fine jets from the nozzle. However, the process is slightly different as it requires a smaller distance between the spinneret and receiver, a lower working voltage, and a higher solution concentration than the electrospinning technique, resulting in the generation of e-jetted filaments having a larger diameter. Nevertheless, they are deposited in a controllable direction. This allows for the preparation of mesh structures with higher dimensional accuracy, providing more precise geometric and topological cues for cell growth. Extraordinary jet stability can be achieved during e-jetting by implementing a secondary electrode [30]. This unique setup enables precise fabrication of a custom design, allowing for tight control over the topographic characteristics and pore size of the artificial esophageal scaffold.

Lee et al. [65] used secondary electrodes to suppress outward-oriented jet motion. The precise positioning of the deposited fibers is crucial for fabricating the target structure [30].

Considering the multilayered structure of the natural esophagus, 3D fiber scaffolds can be prepared through sequential electrospinning [63] and co-electrospinning [64]. Pham et al. [66] prepared alternating layers using microfibers and nanofibers. Furthermore, sandwich configurations that mimic natural ECM structures can be prepared by adjusting the solution and processing parameters [67].

When a cylinder is directly used as a collector (Fig. 4b), it is necessary to address the instability of electrospinning while synchronizing the movement of the spinneret with the rotation of the cylinder to generate an optimal 3D structure

through coordinated motion. This is known as the "inside–out" preparation method, in which a layer of scaffolds is first printed to form the internal structure and then further layers are accumulated in sequence, thereby simulating the complex multilayer structure of the natural esophagus. D'Amato et al. [34] used a rotating mandrel as the collector (Fig. 4c). The inside–out strategy of electrospinning does not require a 3D printer, due to which the fibers can be easily collected using a rotating mandrel. The key parameters include solution flow rate ($T$), mandrel rotation speed ($V_{rot}$), spinnerett translation velocity ($V_{trans}$), mandrel radius ($r$), and applied voltage. A 3D fiber structure with an ideal catheter length ($L$) and fiber winding angle ($\omega$) can be fabricated.

The winding angle is the angle between the fiber and the centerline that extends along the axial length of the mandrel. The winding angle ($\omega$) is determined using the tangential velocity ($V_{tang}$) and translational velocity ($V_{trans}$) (0°–90°). The tangential velocity (in mm/min) is the rotational speed (r/min) of the mandrel multiplied by its radius. Although only $V_{trans}$ and $V_{rot}$ are required as inputs to the machine code, it is necessary to calculate the effective velocity ($V_{eff}$) to ensure consistency in the experiment. The combined speed of the shafts affects the tensile force of the fibers, which in turn affects the diameter of the fibers [68]. The effective velocity is the resultant velocity of the translational and tangential velocities, as shown in Eqs. (3)–(5):

$$\omega = \arctan\left(\frac{V_{tang}}{V_{trans}}\right), \tag{3}$$

$$V_{tang} = r\left(V_{rot} \cdot 2\pi\right), \tag{4}$$

$$V_{eff} = \sqrt{V_{trans}^2 + V_{tang}^2}. \tag{5}$$

For a given mandrel radius, several possible combinations of rotational and translational speeds can achieve the desired winding angle. In addition to symmetrical cylindrical mandrels, asymmetrical mandrels, which are sometimes used to fabricate scaffolds, facilitate adaptation to surgical implantation techniques [35].

Using the electrowriting technique, researchers successfully fabricated catheters with inner diameters ranging from 0.64 to 25.6 mm [34]. The fiber arrangement and stack height within the tubular catheter can be easily modified by adjusting the manufacturing parameters. They produced poly(glycerol sebacate)/poly(ethylene terephthalate) scaffolds with fiber wrapping angles of 35°, 45°, and 75° [34]. The vessel shared a structural resemblance with the esophagus; however, its collagen fibers were arranged in a spiral orientation rather than an orthogonal orientation [69]. Therefore, solution electrowriting enables the fabrication of biomimetic synthetic vascular grafts for specific physiological locations. Similarly, scaffolds with different fiber winding angles and densities can play distinct roles as artificial esophageal scaffolds. They can be used to create multilayered esophageal scaffolds that fulfill the varying environmental requirements for the proliferation and directional growth of mucosal SECs and myometrofibroblasts.

Artificial esophageal scaffolds created using the electrospinning technology have various structures. The number of layers has expanded from one to two and even three or more [6, 26, 33], and the differing porosity and pore size of each layer make this structure suitable for the attachment and growth of cells at different levels. For instance, Wu et al. [33] prepared a double-layer polyethylene oxide/PU scaffold through circular spinning, which had fiber diameters of (438.14±220.74) nm in the inner layer and (362.35±185.51) nm in the outer layer. The fibers comprising the outer layer were arranged in a circumferential pattern, inducing the differentiation of SMCs, whereas the fibers in the inner layer were randomly arranged. In vitro assays have demonstrated that stem cells can simultaneously differentiate into SECs and SMCs. The three-layer scaffold designed by Soliman et al. [6] supported the angiogenic mesenchymal stem cells (MSCs) on the lumen side, and SMCs were located externally to provide the muscle layer required for peristalsis, with a small pore layer in the middle to separate the two cell populations (Fig. 4c). The fiber diameter of the narrow pore layer was (1.5±1.2) μm, and the pore size was (5.7±0.3) μm. The fiber diameter of the wide pore layer was (8.1±0.7) μm, and the pore size was (23.3±1.0) μm. The middle pore layer acted as a barrier, effectively separating the two cell populations and allowing the spatial arrangement of the growing tissue to resemble that of the natural esophagus. This allowed the medium to diffuse inside and outside the lumen through certain pores.

The combination of the previously mentioned electrospinning technology and 3D printing can aid in the development of scaffolds that more closely resemble the structure of the natural esophagus and exhibit its properties. Researchers used 3D printing to reinforce the sequential ring at the scaffold anastomosis site, thereby producing a hybrid biomedical scaffold that exhibited superior mechanical properties to the original electrospun esophageal scaffold and also retained the optimal fibril arrangement for initial cell attachment [43]. After the implantation of the hybrid artificial esophageal scaffold in the body, the peripheral defect caused by the surgery was completely healed by the second week, with only a slight inflammatory response and minimal granulation tissue observed when the infiltrated host cells entered the scaffold. Moreover, the regeneration of squamous SECs and soft tissues was observed. Researchers used electrospinning and 3D printing to prepare a double-layer artificial esophageal scaffold featuring electrospun

nanofibers on the inner surface of the tube to effectively induce the growth of the mucosal layer and promote cell migration and microsized fibers on the outer surface to provide mechanical strength and flexibility [9]. In vitro experiments demonstrated that most cells were well distributed on the nanofiber structure, and the proliferation of MSCs on the nanofiber structure increased over time.

To summarize, esophageal electrospinning based on the "inside–out" strategy is a versatile and superior technique that allows the development of multilayer structures with ideal fiber diameters and pore sizes. This method can mimic the complex structure of the natural esophagus by controlling processing parameters and solution properties. The concentration range of the solution in electrospinning is 0.286–150 mg/mL, the pore size range of the prepared scaffold is 5.7–29 μm, the Young's modulus is 236.19 MPa, and the ultimate strength is 23.8 MPa. Therefore, the application range of this technology is extensive, and the mechanical properties of the prepared scaffold are significantly improved compared with those of scaffolds prepared using traditional methods such as casting, which can play a supportive role. Several in vivo and in vitro experiments have confirmed that an artificial esophageal scaffold prepared through electrospinning has good cytocompatibility, can promote cell adhesion and proliferation, and can reconstruct the mucosa, submucosa, and muscle layer of the esophagus after implantation. Consequently, this scaffold can exhibit a complete structure similar to that of the natural esophagus. Several artificial esophageal scaffolds can promote blood vessel regeneration around tissues, which is beneficial for the healing of esophageal defects.

## 5.2 3D printing of an esophageal tube based on the "bottom–up" strategy

3D printing, also known as additive manufacturing, is used in tissue engineering due to its flexibility in fabrication, diverse biomaterial options, and ability to incorporate live cells [70, 71]. It has already been used to create scaffolds for bone, vessel, and nerve tissue engineering [72–74]. Based on the materials used, ETE scaffolds fabricated via 3D printing can be categorized into two primary types: pure polymer scaffolds and pure bioink scaffolds (Fig. 5a). Farhat et al. [7] used extrusion to fabricate a scaffold composed of polycaprolactone, poly(caprolactone-co-glycolide), methylcellulose, polyethylene glycol, and glycerol (Fig. 5b). The strength, Young's modulus, and elongation at break of the scaffold closely resembled those of the natural human esophagus [75].

Tan et al. [36] proposed a 3D-bioprinted scaffold consisting of a thin encapsulation of poly(D, L-lactic-co-glycolic acid) porous microspheres and an agarose–collagen composite hydrogel that was seeded and expanded in stirred flasks before printing. The final result was a ring structure with a diameter of 1.5 cm and a height of 0.55 cm (Fig. 5c). The cell spheroids had a strong ability to stimulate cell attachment and proliferation during the preprinting step and demonstrated an excellent ability to support cell viability 14 d after printing. Although this was a groundbreaking study on ETE using cell-loaded bioinks, this method could only produce structures of <0.55 cm in height; when longer fragments were printed, the structure collapsed [76–79].

Similarly, Nam et al. developed a multilayer esophageal substitute using extrusion-based 3D bioprinting (Fig. 5d) [8]. They created a polycaprolactone (PCL) tubular structure using the "dragging technique," which leveraged the stretching behavior of viscoelastic materials. This method enabled precise control of hole size and shape in a single extrusion step, providing greater flexibility in the design of the holder. To replicate the complex structure of the natural esophagus, the fabricated tube was filled with acellular bioinks derived from the esophageal mucosal and muscle layers [80].

In addition to traditional 3D printing methods, Takeoka et al. [44] and Taniguchi et al. [81] used the Kenzan technique to fabricate a multicellular esophageal substitute. By using a bio-3D printing system and predesigned structural models, cell beads were individually placed on fine needles arranged in a 3×16-needle array. After printing, the structures were incubated in a bioreactor at 37 °C for one week to allow the spheroids to fuse gradually. The cells were then cultured for an additional three weeks to promote self-organization (Fig. 5e). This technique can be used to create artificial tracheal scaffolds. In vivo analysis revealed complete epithelialization of the lumen surface after implantation, with SMCs remaining outside the epithelial layer. Nonetheless, this approach has limitations, such as a lower mechanical strength (0.3 N compared with 0.5 N for the natural esophagus), which reduces durability. In addition, the production of human-sized esophageal structures requires a substantial number of cells, making the process less practical.

Overall, although 3D bioprinting of artificial esophageal tubular scaffolds is a novel and promising approach, it cannot precisely mimic the complex structural and functional characteristics of the natural esophagus. Most researchers use extrusion-based 3D printing to print tubular structures, either as pure polymer scaffolds or as pure bioink scaffolds. The mechanical properties of such tubular structures are continually improving and therefore gradually approaching those of the natural esophagus. Most polymer scaffolds require seeding with various types of cells, including epithelial, muscle, and fibroblast cells, to promote esophageal tissue regeneration. Nevertheless, 3D-bioprinted esophageal scaffolds exhibit several limitations. For instance, the structure of the esophageal surface cannot be perfectly simulated due to the insufficient accuracy of the printed surface. Furthermore, the low interlaminar bonding strength of

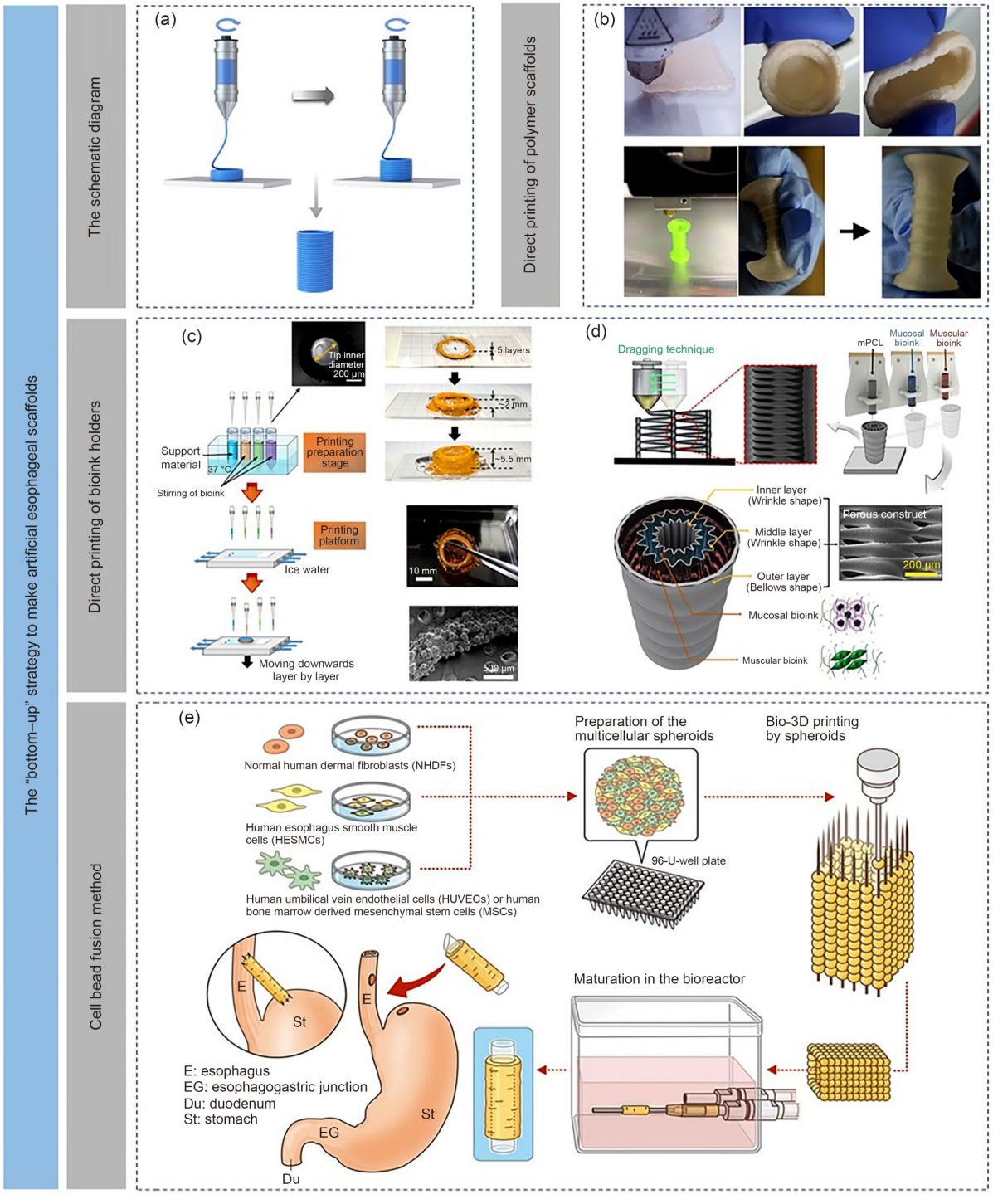


**Fig. 5** The "bottom–up" strategy to create artificial esophageal scaffolds. (a) Schematic of the "bottom–up" strategy. (b) Direct printing of polymer scaffolds. Reproduced from [7] (licensed under CC BY-NC 4.0) and [37] (with permission from Acta Materialia Inc.). (c) Direct printing of bioink holders. Reproduced from [36], licensed under CC BY 4.0. (d) A 3D-printed scaffold is used as the mold to fill with bioink. Reproduced from [8], licensed under CC BY 4.0. (e) Steps and processes for creating artificial esophageal scaffolds using the cell bead fusion method. Reproduced from [44], licensed under CC BY 4.0

the scaffold affects its mechanical properties and stability. Moreover, although the biocompatibility of the selected material may be good, there is no assurance against potential cytotoxicity or that toxic substances will be released during degradation. Therefore, although direct printing of cell microspheres is a promising method, it is necessary to address their structural instability and tendency to collapse by improving the 3D printing technology.

## 6 Regulation cues of tubular scaffolds for functional esophageal cell growth

### 6.1 Topological cues for directing muscle cell alignment

The muscle layer plays a vital role in maintaining the contraction function of the esophagus, and the endocircular and exolongitudinal structure is a special feature of the muscle layer. Shen et al. [82] investigated vascular SMCs and demonstrated that only directionally grown SMCs exhibited contractile function as they were in a contractile phenotype. Under this phenotype, the cells contain a large amount of α-SMA. Conversely, when SMCs grow in random directions, they lose their contractility, transitioning from a "contractile phenotype" to a "synthetic phenotype." In other words, they proliferate into more cells. Hence, the key to ETE scaffold design is controlling the directional growth of muscle cells, ensuring that they remain under the contractile phenotype. ETE scaffolds, similar to the natural ECM, can affect cell growth through topological cues [83], a process known as "contact guidance." When cells come into contact with scaffolds, they can sense the structure and morphology through integrin receptors across the membrane and remodel the actin backbone within the cell, thereby changing the shape of the cell. Radisic and collaborators [84] used grooved polyethylene-based carbonate sheets to guide the directional growth of fibroblasts and cardiomyocytes. In addition, by comparing the effects of different groove widths on fibroblast growth, Bashir and collaborators [85] demonstrated that cells were guided toward directional growth when the groove width was <100 μm. Therefore, ETE scaffolds typically possess narrow topological features that guide directional cell growth.

As depicted in Fig. 6a, researchers applied microgrooves to guide cells in a uniform growth direction. The small microgroove width provides the topological cue required for directional cell growth. Zhu and collaborators [21] used the casting method to prepare PU scaffolds with perpendicular grooves on both sides of the surface, successfully achieving the directional growth of SMCs. They constructed a bilayer scaffold using a combination of casting and hydrogel deposition and cultured esophageal SMCs and SECs on the two layers [9]. In addition to casting, E-jetting is another method for guiding directional cell growth. E-jetted microfibers have been adopted as a key feature [86, 87]. E-jetting, also known as near-field electrospinning or direct writing, can be used to fabricate degradable materials into microfibers with high mechanical strengths, regular arrangements, and microwidths. Moreover, these fibers can be stacked into porous scaffolds. He et al. [88] stably fabricated a PCL scaffold with a fiber diameter of 10 μm using e-jetting and demonstrated its ability to induce the directional growth of cardiomyocytes. They prepared PCL scaffolds with fiber

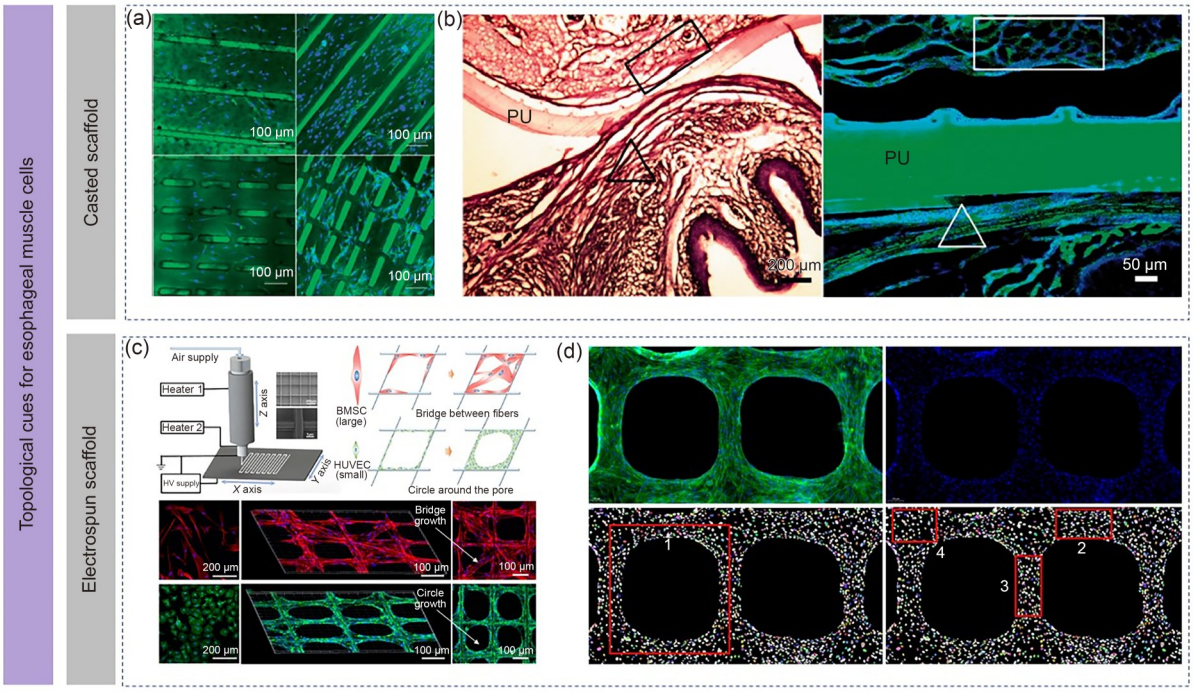


**Fig. 6** Topological cues of casted and electrospun scaffolds for the growth of esophageal muscle cells. Casted scaffold: (a) groove-guided cell-directed growth; (b) immunostaining blot of muscle cells. Reproduced from [21], licensed under CC BY 4.0. Electrospun scaffold: (c) effect of the grid scaffold on the direction of cell growth (reproduced from [89], licensed under CC BY 4.0); (d) quantitative statistical analysis of nuclei angle distribution based on the circle growth (reproduced from [86], licensed under CC BY-NC-ND 4.0)

diameters ranging from 3 to 22 μm using e-jetting and demonstrated their ability to guide the directed growth of stem and vascular endothelial cells [89]. Furthermore, muscle cells can be stained via immunostaining (Fig. 6b) [9, 21].

As e-jetting is a type of additive manufacturing technique, the shape and features of the e-jetted scaffold can be controlled to a significant degree of freedom. For instance, the width of fibers and the size of the pores enclosed by fibers can be controlled. Based on different combinations of fiber width and pore size, the cells can bridge through the center of the pores (bridge growth) or grow on the circumference of the pores (circle growth) (Fig. 6c) [89]. In addition, the e-jetted fibers can induce stem cells to undergo circular growth [90]. Wu et al. [86, 87] quantitatively analyzed the distribution of nuclear angle orientation under circular growth using an artificial intelligence statistical tool. Their results demonstrated that a large pore size can improve the uniformity of the angle distribution of the cell nucleus. When the pore size was small, the cells were easily influenced by the neighboring perpendicular fibers, resulting in a less uniform distribution (Fig. 6d).

### 6.2 Topological cues for the tight junctions of SECs

In addition to the muscle layer, the mucosal layer is vital for the complete function of the esophagus. As it comes into direct contact with food, it functions as a barrier to protect the esophagus from any harm caused by heat, scratches, or even poison. Unlike the keratinizing epidermis of the skin, the epithelium of the esophagus is nonkeratinized due to the low external mechanical load and low external stimulus. The cells at the bottom of the esophageal epithelium are known as basal cells. The basal cell layer is only 1–3-cell thick, occupying 10%–15% of the epithelium. However, in epithelial hyperplasia, the basal cell layer constitutes >15% of the total thickness. The basal cells are highly proliferative and can migrate to the surface of the epithelium to replenish the cells that frequently experience wear and tear. During the movement process, the cells become differentiated, flat, and less proliferative [91]. This loss–replenishment balance of the epithelium is known as epithelial homeostasis, a protective mechanism that limits the colonization and invasion of microorganisms adhering to the mucosal surface. In humans, the median regeneration period of the esophageal epithelium is approximately 21 d [92]. Epithelium homeostasis can also occur in other digestive organs, such as the small intestine [93].

As shown in Fig. 7a, SECs cultured on electrospun films exhibit a squamous phenotype and reach complete confluence to cover the entire film surface [26]. Cytokeratin-14 is a member of type I keratin and a component of the cytoskeleton of SECs. Moreover, filamentous actin and vinculin are key components and have been considered markers of SECs [25]. Sparse cells cannot form a barrier; only a large number of SECs can form tight junctions (Figs. 7b and 7c). Once these tight junctions are formed, myosin forces are generated between the cells. Thus, cells in confluence form a barrier with low permeability that can prevent the transport of macromolecular drugs [94].

### 6.3 Chemical cues for the coculture of muscle cells and SECs

Another problem with ETE is that fibroblast coculture is not considered. According to skin and myocardial tissue engineering, the epidermal growth factor (EGF) and transforming growth factor-β (TGF-β) secreted by fibroblasts can promote the proliferation and differentiation of epidermal cells and SMCs, respectively [10, 95]. Furthermore, both the α-SMA of fibroblasts and the collagen secreted by fibroblasts play a vital role in increasing tissue elasticity [96], a process that requires the fibroblasts to be oriented and elongated. This is because the elongation state activates the expression of the TGF-β receptor and connective tissue growth factor/CCN2 in fibroblasts, upregulating the secretion of TGF-β, which in turn promotes the expression of α-SMA and increases cell contractility [97]. Simultaneously, the upregulation of TGF-β can increase type I collagen secretion and decrease matrix metalloproteinase (MMP) secretion. A decrease in MMP content reduces the rate of collagen degradation [98].

Wu and collaborators cocultured SECs and fibroblasts using a cryospun Janus film, with the SECs and fibroblasts cultured on different sides of the film. The film was a semipermeable membrane that prevented cell invasion and allowed paracrine action between SECs and fibroblasts. Consequently, the EGF secreted by the fibroblasts increased the secretion of Mcl-1 and c-Myc RNA by the SECs, which increased the ability of the cells to cope with an adverse environment and regulate cell proliferation (Fig. 7d) [99]. Hence, an ideal ETE scaffold should regenerate both the mucosal and muscle layers (Fig. 7e) [100].

## 7 Conclusions and outlooks

### 7.1 Conclusions

The esophagus is a specialized organ with a tubular shape and multiple layers. Due to their complex structures and functions, ETE scaffolds have received relatively less research attention than organs such as the bone, skin, and vessels. Nevertheless, ETE scaffold fabrication is a promising method based on the efforts of numerous researchers. This

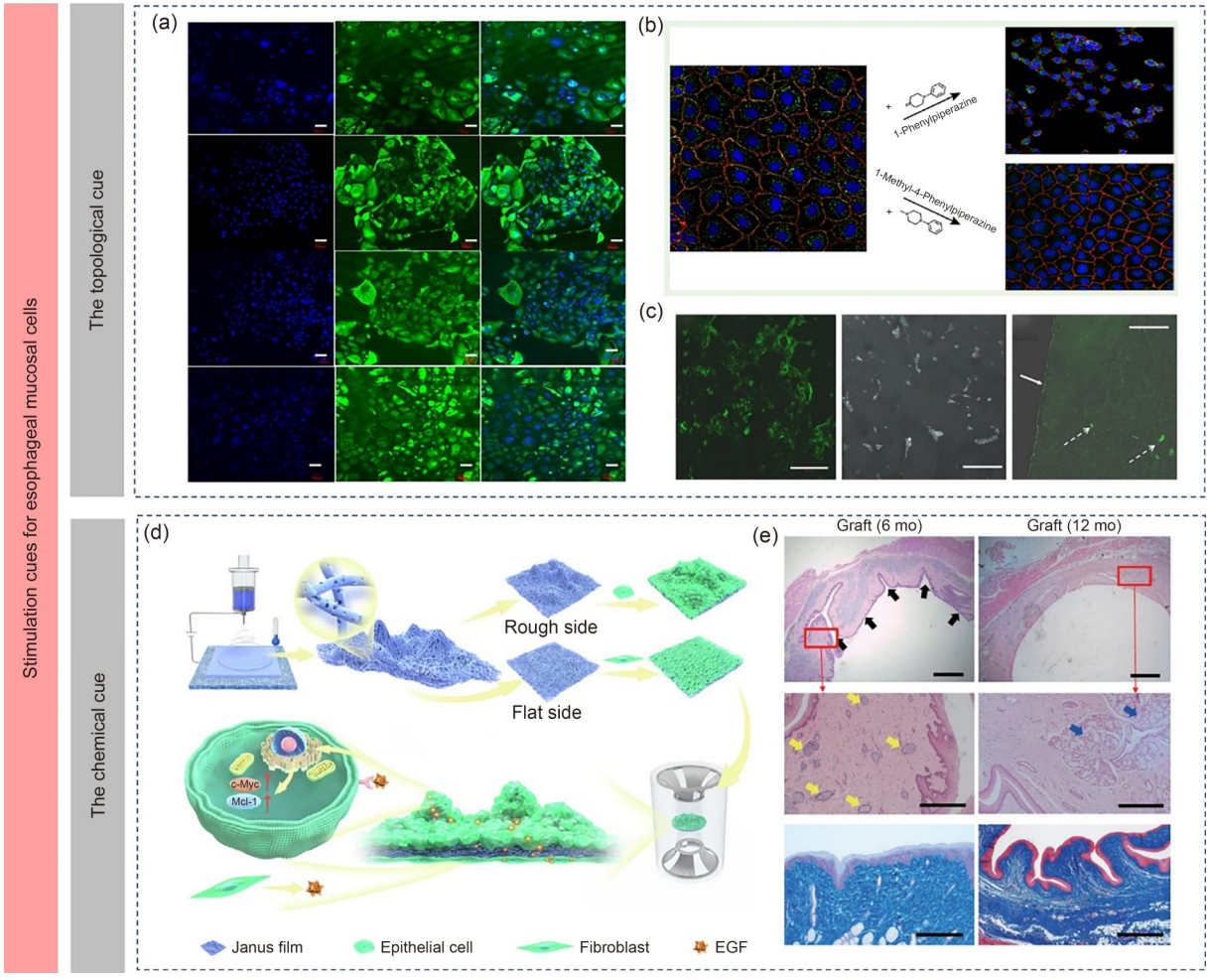


**Fig. 7** Effects of scaffold features on cells in the esophageal mucosal layer. Topological cue: (a) staining of nuclei with cytokeratin and its complexes showed that endothelial cells cultured on coated PCL/SF scaffolds not only exhibited an epithelial phenotype but also covered the entire scaffolding surface (reproduced from [26], with permission from the American Chemical Society); (b) the tight junction morphology that normal epithelial cells need to achieve (reproduced from [94], with permission from the American Chemical Society); (c) morphology of epithelial cells living on the surface of the scaffold, where a continuous layer of epithelial cells was found to have grown on top of the scaffold (reproduced from [18], with permission from Elsevier B.V.). Chemical cue: (d) paracrine interaction between cells—fibroblasts can secrete epidermal growth factor (EGF), which can promote epithelial cell growth (reproduced from [99], licensed under CC BY 4.0); (e) regeneration of mucosal and muscular layers (reproduced from [100], with permission from the Korean Society of Otorhinolaryngology-Head and Neck Surgery)

review has summarized the fabrication process of ETE scaffolds and the stimulation cues for cell growth.

1. Fabrication methods for ETE scaffolds

The five major fabrication methods for ETE tubular scaffolds are decellularization, casting, electrospinning, 3D bioprinting, and pin-frogging. Decellularization is similar to allografts but involves the removal of all original cells. The material used is a natural esophagus from an animal. The advantage of this strategy is that it retains natural proteins, thereby providing a friendly microenvironment for cells [14]. However, its disadvantages include limited sources, high complexity, high expense, and poor mechanical properties. Casting has been used for a long time in ETE, and its advantages include its simple process and wide selection of materials. Nonetheless, the casting mold can only produce a solid tube with no porosity, and the structural features can only be fabricated on the inner and outer surfaces of the tube [24]. Electrospinning is the most widely used technique for the fabrication of these tubular scaffolds owing to its simplicity in creating multilayer structures using the "inside–out" strategy. Nevertheless, it provides limited precise control of nanofibers. 3D bioprinting is a promising fabrication technique that has undergone significant advances recently. It directly applies biocompatible hydrogels and even live cells as bioinks. However, it can exhibit poor mechanical properties and structural fidelity [36], which hinder the stimulation of cell growth through topological cues (topotaxis) or stiffness cues (durotaxis). Pin-frogging is a type of material-free fabrication technique that only uses cell spheroids. Although it does not require degradation

of the biomaterial, it is extremely expensive and time-consuming [81].

2. Stimulation cues of the scaffold for cell growth

Although functional resemblance is more essential than shape resemblance in ETE tubes, shape resemblance is the premise of functional resemblance. The muscle and mucosal layers have special requirements for sustaining normal esophageal function. Muscle cells must be elongated to achieve elasticity, and SECs require tight junctions between them to function as barriers. The topology and stiffness of scaffolds are vital cues for cell growth and behavior. For muscle cells, a narrow groove or thin fiber is used to induce cell alignment [21]. A flat surface is used for the confluent growth of SECs. Chemical cues also play a crucial role in cell growth. The EGF secreted by fibroblasts can induce the growth of SECs and the secretion of Mcl-1 and c-Myc.

## 7.2 Outlooks

An ETE tubular structure is promising in the field of esophageal repair and reconstruction; however, its accurate fabrication is complex. This review summarizes the existing fabrication methods along with stimulation cues required for scaffolds to promote esophageal cell growth. Nevertheless, several concerns remain regarding the design and fabrication of ETE scaffolds and should be addressed in future studies.

The first concern is the leakage and porosity of the esophageal tubular scaffold. Porosity is a basic requirement for tissue engineering scaffolds, as it induces cell growth, oxygen exchange, and blood perfusion. However, high porosity may cause leakage, which is a potentially fatal complication for the esophageal tube. Avoiding leakage while maintaining high porosity is a challenge. A possible solution could be the growth of confluence cells, which can produce an intact cylinder to prevent leakage. Nevertheless, this solution may introduce a second problem as described below.

The second concern is the elasticity and proliferation of SMCs. SMCs have two different phenotypes, namely, "contractile" and "synthetic." They exhibit only contraction when they stop proliferating [101]. Hence, inducing muscle cell elongation while maintaining the number of cells is a challenge. A possible solution is to initially proliferate cells and then change their phenotype to the one that promotes contraction.

The third concern is the balance between the biocompatibility and structural fidelity of biomaterials. The biomaterials used in ETE can be broadly categorized into two major types: polymers and hydrogels. Polymers possess sufficient strength to provide topological cues but poor biodegradability, whereas hydrogels possess better biodegradability but poor mechanical strength.

The following two strategies can be used to address these three concerns. The first approach involves preparation of a scaffold using polymer biomaterials to ensure its shape and strength, as well as the mechanical cues it provides. Subsequently, the surface and interior of the scaffold are seeded with cells to prevent leakage. The cells are induced to differentiate into a scalable phenotype, which improves their orientation, and the remaining part of the polymer material ultimately forms a perfect esophageal scaffold that closely resembles the natural esophagus. The main aim of this approach is to develop polymeric materials with improved biodegradability. The second approach involves directly printing an artificial esophageal scaffold using a hydrogel biomaterial containing cells and then using an external field, such as an electric, magnetic, or stress field, to stimulate cell growth. Nevertheless, the quality of the mechanical properties of scaffolds prepared using this method depends on several post-treatment processes, such as light- or pH-induced crosslinking.

The preparation of other hollow tubular scaffolds, such as blood vessels and the trachea, can be examined to gain inspiration for developing esophageal scaffolds. The physiological structures of the esophagus and blood vessels are relatively similar; however, the structures and materials of the trachea and esophagus differ significantly and feature cartilage and muscle. Therefore, we can learn from established methods and the latest advances in vascular tissue engineering, scaffolding [17, 102–104]. For instance, Yao et al. [24] prepared tubular vascular scaffolds using the casting method and used electrospinning to create a bilayer structure on the outer layer of the scaffold. The prepared tubular scaffold exhibited a smooth and dense inner surface accompanied by a porous and fluffy outer surface. The smooth, dense inner surface prevented blood leakage, whereas the porous, fluffy outer surface aided in the regeneration and growth of vascular SMCs. The interconnected microporous structure between the inner and outer layers of the scaffold enabled extensive blood penetration into the inner layer of the scaffold wall, providing a favorable microenvironment for the adhesion of endothelial cells [24]. This approach addresses the previously mentioned concerns of leakage, porosity, and cell growth. The ETE method can be used to prepare similar multilayer structures, thereby addressing the first and second concerns. The third concern should focus on the material of the scaffold, as the development of new materials and the modification of current materials may become a reasonable solution.

To summarize, ETE is highly promising in future applications, despite several concerns that require attention. Based on the experience of adjacent fields and with the continuous development of materials and technologies, we can anticipate that ETE will develop in an unprecedented manner.

**Acknowledgements** The authors would like to thank the support from the National Natural Science Foundation of China (No.

82472440), Hubei Provincial Natural Science Foundation of China (No. 2023AFB141), the National Medical Products Administration Key Laboratory for Dental Materials (No. PKUSS20240401), and the Cross-Research Support Program from Huazhong University of Science and Technology.

**Author contributions** XYZ: writing—original draft and writing—review & editing. XLZ: supervision and funding acquisition. BW: writing—original draft, writing—review & editing, supervision, and funding acquisition.

## Declarations

**Conflict of interest** The authors declare that they have no conflict of interest.

**Ethical approval** This article does not contain any studies with human or animal subjects performed by any of the authors.

**Use of generative AI tools** No generative AI tools were used in the preparation of this manuscript.

## References

1. Giannakis M, Peters U (2021) Esophageal cancer mutational signatures around the world. *Nat Genet* 53(11):1522–1523. https://doi.org/10.1038/s41588-021-00958-0
2. Chokshi NK, Guner YS, Ndiforchu F et al (2009) Combined laparoscopic and thoracoscopic esophagectomy and gastric pull-up in a child. *J Laparoendosc Adv Surg Tech A* 19(Suppl 1): S197–S200. https://doi.org/10.1089/lap.2008.0222.supp
3. Siegel RL, Giaquinto AN, Jemal A (2024) Cancer statistics, 2024. *CA Cancer J Clin* 74(1):12–49. https://doi.org/10.3322/caac.21820
4. Qin JF, Zhao JP, Wu Y et al (2022) Chitosan/collagen layer-by-layer deposition for improving the esophageal regeneration ability of nanofibrous mats. *Carbohydr Polym* 286:119269. https://doi.org/10.1016/j.carbpol.2022.119269
5. Zhuravleva M, Gilazieva Z, Grigoriev TE et al (2019) *In vitro* assessment of electrospun polyamide-6 scaffolds for esophageal tissue engineering. *J Biomed Mater Res B Appl Biomater* 107(2): 253–268. https://doi.org/10.1002/jbm.b.34116
6. Soliman S, Laurent J, Kalenjian L et al (2019) A multilayer scaffold design with spatial arrangement of cells to modulate esophageal tissue growth. *J Biomed Mater Res Part B Appl Biomater* 107(2):324–331. https://doi.org/10.1002/jbm.b.34124
7. Farhat W, Ayollo D, Arakelian L et al (2022) Biofabrication of an esophageal tissue construct from a polymer blend using 3D extrusion-based printing. *Adv Eng Mater* 24(9):2200096. https://doi.org/10.1002/adem.202200096
8. Nam H, Jeong HJ, Jo Y et al (2020) Multi-layered free-form 3D cell-printed tubular construct with decellularized inner and outer esophageal tissue-derived bioinks. *Sci Rep* 10(1):7255. https://doi.org/10.1038/s41598-020-64049-6
9. Kim IG, Wu YR, Park SA et al (2019) Tissue-engineered esophagus via bioreactor cultivation for circumferential esophageal reconstruction. *Tissue Eng Part A* 25(21–22):1478–1492. https://doi.org/10.1089/ten.TEA.2018.0277
10. Brasseur JG, Nicosia MA, Pal A et al (2007) Function of longitudinal *vs* circular muscle fibers in esophageal peristalsis, deduced with mathematical modeling. *World J Gastroenterol* 13(9):1335–1346
11. Tan JY, Chua CK, Leong KF et al (2012) Esophageal tissue engineering: an in-depth review on scaffold design. *Biotechnol Bioeng* 109(1):1–15. https://doi.org/10.1002/bit.23323
12. Berman EF (1952) The experimental replacement of portions of the esophagus by a plastic tube. *Ann Surg* 135(3):337–343. https://doi.org/10.1097/00000658-195203000-00007
13. Levenson G, Berger A, Demma J et al (2022) Circumferential esophageal replacement by a decellularized esophageal matrix in a porcine model. *Surgery* 171(2):384–392. https://doi.org/10.1016/j.surg.2021.07.009
14. Urbani L, Camilli C, Phylactopoulos DE et al (2018) Multistage bioengineering of a layered oesophagus with in vitro expanded muscle and epithelial adult progenitors. *Nat Commun* 9: 4286. https://doi.org/10.1038/s41467-018-06385-w
15. Giobbe GG, Zambon A, Vetralla M et al (2018) Preservation over time of dried acellular esophageal matrix. *Biomed Phys Eng Express* 4(6):065021. https://doi.org/10.1088/2057-1976/aae4ff
16. Marzaro M, Algeri M, Tomao L et al (2020) Successful muscle regeneration by a homologous microperforated scaffold seeded with autologous mesenchymal stromal cells in a porcine esophageal substitution model. *Therap Adv Gastroenterol* 13:1–12. https://doi.org/10.1177/1756284820923220
17. Sugimura Y, Chekhoeva A, Oyama K et al (2020) Controlled autologous recellularization and inhibited degeneration of decellularized vascular implants by side-specific coating with stromal cell-derived factor 1α and fibronectin. *Biomed Mater* 15(3):035013. https://doi.org/10.1088/1748-605X/ab54e3
18. Zhu YB, Ong WF, Chan W et al (2010) Construct of asymmetrical scaffold and primary cells for tissue engineered esophagus. *Mater Sci Eng C* 30(3):400–406. https://doi.org/10.1016/j.msec.2009.12.009
19. Seth A, Chung YG, Gil ES et al (2013) The performance of silk scaffolds in a rat model of augmentation cystoplasty. *Biomaterials* 34(20):4758–4765. https://doi.org/10.1016/j.biomaterials.2013.03.038
20. Hou L, Jin JC, Lv JJ et al (2015) Constitution and in vivo test of micro-porous tubular scaffold for esophageal tissue engineering. *J Biomater Appl* 30(5):568–578. https://doi.org/10.1177/0885328215596285
21. Hou L, Gong CF, Zhu YB (2016) In vitro construction and in vivo regeneration of esophageal bilamellar muscle tissue. *J Biomater Appl* 30(9):1373–1384. https://doi.org/10.1177/0885328215627585
22. Algarrahi K, Franck D, Savarino A et al (2018) Bilayer silk fibroin grafts support functional oesophageal repair in a rodent model of caustic injury. *J Tissue Eng Regen Med* 12(2): e1068–e1075. https://doi.org/10.1002/term.2434
23. Hou RX, Wang XY, Wei QQ et al (2019) Biological properties of a bionic scaffold for esophageal tissue engineering research. *Colloids Surf B Biointerfaces* 179:208–217. https://doi.org/10.1016/j.colsurfb.2019.03.072
24. Yao WC, Gu HB, Hong T et al (2020) A bi-layered tubular scaffold for effective anti-coagulant in vascular tissue engineering. *Mater Des* 194:108943. https://doi.org/10.1016/j.matdes.2020.108943
25. Kuppan P, Sethuraman S, Krishnan UM (2014) Poly(3-hydroxybutyrate-co-3-hydroxyvalerate)-based nanofibrous scaffolds to support functional esophageal epithelial cells towards engineering the esophagus. *J Biomater Sci Polym Ed* 25(6):574–593.

https://doi.org/10.1080/09205063.2014.884427
26. Lv JJ, Chen L, Zhu YB et al (2014) Promoting epithelium regeneration for esophageal tissue engineering through basement membrane reconstitution. *ACS Appl Mater Interfaces* 6(7): 4954–4964. https://doi.org/10.1021/am4059809
27. Jensen T, Blanchette A, Vadasz S et al (2015) Biomimetic and synthetic esophageal tissue engineering. *Biomaterials* 57:133–141. https://doi.org/10.1016/j.biomaterials.2015.04.004
28. Tan YJ, Yeong WY, Tan XP et al (2016) Characterization, mechanical behavior and *in vitro* evaluation of a melt-drawn scaffold for esophageal tissue engineering. *J Mech Behav Biomed Mater* 57:246–259. https://doi.org/10.1016/j.jmbbm.2015.12.015
29. Barron MR, Blanco EW, Aho JM et al (2018) Full-thickness oesophageal regeneration in pig using a polyurethane mucosal cell seeded graft. *J Tissue Eng Regen Med* 12(1):175–185. https://doi.org/10.1002/term.2386
30. Jordahl JH, Solorio L, Sun HL et al (2018) 3D jet writing: functional microtissues based on tessellated scaffold architectures. *Adv Mater* 30(14):1707196. https://doi.org/10.1002/adma.201707196
31. La Francesca S, Aho JM, Barron MR et al (2018) Long-term regeneration and remodeling of the pig esophagus after circumferential resection using a retrievable synthetic scaffold carrying autologous cells. *Sci Rep* 8(1):4123. https://doi.org/10.1038/s41598-018-22401-x
32. Syed O, Kim JH, Keskin-Erdogan Z et al (2019) SIS/aligned fibre scaffold designed to meet layered oesophageal tissue complexity and properties. *Acta Biomater* 99:181–195. https://doi.org/10.1016/j.actbio.2019.08.015
33. Wu Y, Kang YG, Kim IG et al (2019) Mechanical stimuli enhance simultaneous differentiation into oesophageal cell lineages in a double-layered tubular scaffold. *J Tissue Eng Regen Med* 13(8):1394–1405. https://doi.org/10.1002/term.2881
34. D'Amato AR, Ding XC, Wang YD (2021) Using solution electrowriting to control the properties of tubular fibrous conduits. *ACS Biomater Sci Eng* 7(2):400–407. https://doi.org/10.1021/acsbiomaterials.0c01419
35. Pisani S, Croce S, Mauramati S et al (2022) Engineered full thickness electrospun scaffold for esophageal tissue regeneration: from in vitro to in vivo approach. *Pharmaceutics* 14(2):252. https://doi.org/10.3390/pharmaceutics14020252
36. Tan YJ, Tan XP, Yeong WY et al (2016) Hybrid microscaffold-based 3D bioprinting of multi-cellular constructs with high compressive strength: a new biofabrication strategy. *Sci Rep* 6: 39140. https://doi.org/10.1038/srep39140
37. Lin MH, Firoozi N, Tsai CT et al (2019) 3D-printed flexible polymer stents for potential applications in inoperable esophageal malignancies. *Acta Biomater* 83:119–129. https://doi.org/10.1016/j.actbio.2018.10.035
38. Yeleswarapu S, Chameettachal S, Pati F (2021) Integrated 3D printing-based framework—a strategy to fabricate tubular structures with mechanocompromised hydrogels. *ACS Appl Bio Mater* 4(9):6982–6992. https://doi.org/10.1021/acsabm.1c00644
39. Ding Y, Fu R, Collins CP et al (2022) 3D-printed radiopaque bioresorbable stents to improve device visualization. *Adv Healthc Mater* 11(23):e2201955. https://doi.org/10.1002/adhm.202201955
40. Zhu T, Hu Y, Cui HT et al (2024) 3D multispheroid assembly strategies towards tissue engineering and disease modeling. *Adv Healthc Mater* 13(23):2400957. https://doi.org/10.1002/adhm.202400957
41. Murata D, Arai K, Nakayama K (2020) Scaffold-free bio-3D printing using spheroids as "bio-inks" for tissue (Re-)construction and drug response tests. *Adv Healthc Mater* 9(15): e1901831. https://doi.org/10.1002/adhm.201901831
42. Poghosyan T, Sfeir R, Michaud L et al (2015) Circumferential esophageal replacement using a tube-shaped tissue-engineered substitute: an experimental study in minipigs. *Surgery* 158(1): 266–277. https://doi.org/10.1016/j.surg.2015.01.020
43. Chung EJ, Ju HW, Yeon YK et al (2018) Development of an omentum-cultured oesophageal scaffold reinforced by a 3D-printed ring: feasibility of an *in vivo* bioreactor. *Artif Cells Nanomed Biotechnol* 46(Suppl 1):885–895. https://doi.org/10.1080/21691401.2018.1439039
44. Takeoka Y, Matsumoto K, Taniguchi D et al (2019) Regeneration of esophagus using a scaffold-free biomimetic structure created with bio-three-dimensional printing. *PLoS ONE* 14(3):e0211339. https://doi.org/10.1371/journal.pone.0211339
45. Luc G, Durand M, Collet D et al (2014) Esophageal tissue engineering. *Expert Rev Med Devices* 11(2):225–241. https://doi.org/10.1586/17434440.2014.870470
46. Badylak S, Meurling S, Chen MK et al (2000) Resorbable bioscaffold for esophageal repair in a dog model. *J Pediatr Surg* 35(7):1097–1103. https://doi.org/10.1053/jpsu.2000.7834
47. Badylak SF, Kochupura PV, Cohen IS et al (2006) The use of extracellular matrix as an inductive scaffold for the partial replacement of functional myocardium. *Cell Transplant* 15(Suppl 1): S29–S40. https://doi.org/10.3727/000000006783982368
48. Lopes MF, Cabrita A, Ilharco J et al (2006) Esophageal replacement in rat using porcine intestinal submucosa as a patch or a tube-shaped graft. *Dis Esophagus* 19(4):254–259. https://doi.org/10.1111/j.1442-2050.2006.00574.x
49. Lopes MF, Cabrita A, Ilharco J et al (2006) Grafts of porcine intestinal submucosa for repair of cervical and abdominal esophageal defects in the rat. *J Investig Surg* 19(2):105–111. https://doi.org/10.1080/08941930600569621
50. Urita Y, Komuro H, Chen GP et al (2007) Regeneration of the esophagus using gastric acellular matrix: an experimental study in a rat model. *Pediatr Surg Int* 23(1):21–26. https://doi.org/10.1007/s00383-006-1799-0
51. Nakase Y, Nakamura T, Kin S et al (2008) Intrathoracic esophageal replacement by in situ tissue-engineered esophagus. *J Thorac Cardiovasc Surg* 136(4):850–859. https://doi.org/10.1016/j.jtcvs.2008.05.027
52. Doede T, Bondartschuk M, Joerck C et al (2009) Unsuccessful alloplastic esophageal replacement with porcine small intestinal submucosa. *Artif Organs* 33(4):328–333. https://doi.org/10.1111/j.1525-1594.2009.00727.x
53. Beckstead BL, Pan S, Bhrany AD et al (2005) Esophageal epithelial cell interaction with synthetic and natural scaffolds for tissue engineering. *Biomaterials* 26(31):6217–6228. https://doi.org/10.1016/j.biomaterials.2005.04.010
54. Bhrany AD, Lien CJ, Beckstead BL et al (2008) Crosslinking of an oesophagus acellular matrix tissue scaffold. *J Tissue Eng Regen Med* 2(6):365–372. https://doi.org/10.1002/term.105
55. Arakelian L, Caille C, Faivre L et al (2019) A clinical-grade acellular matrix for esophageal replacement. *J Tissue Eng Regen Med* 13(12):2191–2203. https://doi.org/10.1002/term.2983
56. Gong YH, Ma ZW, Gao CY et al (2006) Specially elaborated

thermally induced phase separation to fabricate poly(L-lactic acid) scaffolds with ultra large pores and good interconnectivity. *J Appl Polym Sci* 101(5):3336–3342. https://doi.org/10.1002/app.23931
57. Song SW, Torkelson JM (1995) Coarsening effects on the formation of microporous membranes produced via thermally induced phase separation of polystyrene-cyclohexanol solutions. *J Membr Sci* 98(3):209–222. https://doi.org/10.1016/0376-7388(94)00189-6
58. Reneker DH, Chun I (1996) Nanometre diameter fibres of polymer, produced by electrospinning. *Nanotechnology* 7(3):216. https://doi.org/10.1088/0957-4484/7/3/009
59. Fong H, Chun I, Reneker DH (1999) Beaded nanofibers formed during electrospinning. *Polymer* 40:4585–4592. https://doi.org/10.1016/S0032-3861(99)00068-3
60. Sun B, Long YZ, Zhang HD et al (2014) Advances in three-dimensional nanofibrous macrostructures via electrospinning. *Prog Polym Sci* 39(5):862–890. https://doi.org/10.1016/j.progpolymsci.2013.06.002
61. Lastow O, Balachandran W (2006) Numerical simulation of electrohydrodynamic (EHD) atomization. *J Electrostat* 64(12): 850–859. https://doi.org/10.1016/j.elstat.2006.02.006
62. Rahmanpour M, Ebrahimi R, Pourrajabian A (2017) Numerical simulation of two-phase electrohydrodynamic of stable Taylor cone–jet using a volume-of-fluid approach. *J Braz Soc Mech Sci Eng* 39(11):4443–4453. https://doi.org/10.1007/s40430-017-0832-7
63. Woodfield TBF, Van Blitterswijk CA, De Wijn J et al (2005) Polymer scaffolds fabricated with pore-size gradients as a model for studying the zonal organization within tissue-engineered cartilage constructs. *Tissue Eng* 11(9–10):1297–1311. https://doi.org/10.1089/ten.2005.11.1297
64. Soliman S, Pagliari S, Rinaldi A et al (2010) Multiscale three-dimensional scaffolds for soft tissue engineering via multimodal electrospinning. *Acta Biomater* 6(4):1227–1237. https://doi.org/10.1016/j.actbio.2009.10.051
65. Lee J, Lee SY, Jang J et al (2012) Fabrication of patterned nanofibrous mats using direct-write electrospinning. *Langmuir* 28(18): 7267–7275. https://doi.org/10.1021/la3009249
66. Pham QP, Sharma U, Mikos AG (2006) Electrospun poly(ε-caprolactone) microfiber and multilayer nanofiber/microfiber scaffolds: characterization of scaffolds and measurement of cellular infiltration. *Biomacromolecules* 7(10):2796–2805. https://doi.org/10.1021/bm060680j
67. Han D, Gouma PI (2006) Electrospun bioscaffolds that mimic the topology of extracellular matrix. *Nanomed Nanotechnol Biol Med* 2(1):37–41. https://doi.org/10.1016/j.nano.2006.01.002
68. McColl E, Groll J, Jungst T et al (2018) Design and fabrication of melt electrowritten tubes using intuitive software. *Mater Des* 155:46–58. https://doi.org/10.1016/j.matdes.2018.05.036
69. Cyron CJ, Humphrey JD (2015) Preferred fiber orientations in healthy arteries and veins understood from netting analysis. *Math Mech Solids* 20(6):680–696. https://doi.org/10.1177/1081286514551495
70. Meng ZJ, Mu XD, He JK et al (2023) Embedding aligned nanofibrous architectures within 3D-printed polycaprolactone scaffolds for directed cellular infiltration and tissue regeneration. *Int J Extreme Manuf* 5(2):025001. https://doi.org/10.1088/2631-7990/acbd6c
71. Ma CY, Zeng QF, Yu LW et al (2023) Preparation and characterization of 3D printed hydroxyapatite-whisker-strengthened hydroxyapatite scaffold coated with biphasic calcium phosphate. *Chin J Mech Eng Addit Manuf Front* 2(4):100097. https://doi.org/10.1016/j.cjmeam.2023.100097
72. Song JQ, Lv BH, Chen WC et al (2023) Advances in 3D printing scaffolds for peripheral nerve and spinal cord injury repair. *Int J Extrem Manuf* 5(3):032008. https://doi.org/10.1088/2631-7990/acde21
73. Zhu H, Yao C, Wei BY et al (2023) 3D printing of functional bioengineered constructs for neural regeneration: a review. *Int J Extrem Manuf* 5(4):042004. https://doi.org/10.1088/2631-7990/ace56c
74. Li H, Hu Y, Tang XP et al (2024) Biomechanical and biological properties of stereolithography-based 3D-printed zirconia interference screws for anterior cruciate ligament reconstruction. *Addit Manuf Front* 3(3):200135. https://doi.org/10.1016/j.amf.2024.200135
75. Egorov VI, Schastlivtsev IV, Prut EV et al (2002) Mechanical properties of the human gastrointestinal tract. *J Biomech* 35(10): 1417–1425. https://doi.org/10.1016/S0021-9290(02)00084-2
76. Hendow EK, Guhmann P, Wright B et al (2016) Biomaterials for hollow organ tissue engineering. *Fibrogenesis Tissue Repair* 9:3. https://doi.org/10.1186/s13069-016-0040-6
77. McCormack A, Highley CB, Leslie NR et al (2020) 3D printing in suspension baths: keeping the promises of bioprinting afloat. *Trends Biotechnol* 38(6):584–593. https://doi.org/10.1016/j.tibtech.2019.12.020
78. Ji S, Almeida E, Guvendiren M (2019) 3D bioprinting of complex channels within cell-laden hydrogels. *Acta Biomater* 95: 214–224. https://doi.org/10.1016/j.actbio.2019.02.038
79. Zou Q, Grottkau BE, He ZX et al (2020) Biofabrication of valentine-shaped heart with a composite hydrogel and sacrificial material. *Mater Sci Eng C* 108:110205. https://doi.org/10.1016/j.msec.2019.110205
80. Farhat W, Chatelain F, Marret A et al (2021) Trends in 3D bioprinting for esophageal tissue repair and reconstruction. *Biomaterials* 267:120465. https://doi.org/10.1016/j.biomaterials.2020.120465
81. Taniguchi D, Matsumoto K, Tsuchiya T et al (2018) Scaffold-free trachea regeneration by tissue engineering with bio-3D printing. *Interact Cardiovasc Thorac Surg* 26(5):745–752. https://doi.org/10.1093/icvts/ivx444
82. Shen JY, Chan-Park MB, He B et al (2006) Three-dimensional microchannels in biodegradable polymeric films for control orientation and phenotype of vascular smooth muscle cells. *Tissue Eng* 12(8):2229–2240. https://doi.org/10.1089/ten.2006.12.2229
83. Ye J, Zhou XY, Huang Z et al (2025) Low-temperature-field-assisted fabrication of cross-scale tissue engineering scaffolds. *Int J Extrem Manuf* 7(2):022011. https://doi.org/10.1088/2631-7990/ad996d
84. Au HTH, Cheng I, Chowdhury MF et al (2007) Interactive effects of surface topography and pulsatile electrical field stimulation on orientation and elongation of fibroblasts and cardiomyocytes. *Biomaterials* 28(29):4277–4293. https://doi.org/10.1016/j.biomaterials.2007.06.001
85. Chan V, Collens MB, Jeong JH et al (2012) Directed cell growth and alignment on protein-patterned 3D hydrogels with stereolithography. *Virtual Phys Prototyp* 7(3):219–228. https://doi.org/10.1080/17452759.2012.709423
86. Deng BC, Huang ZW, Zhang XL et al (2024) Durotaxis and topotaxis orchestrated guidance on cell migration in 3D printed scaffold/hydrogel composite. *Addit Manuf Front* 3(2):200134. https://doi.org/10.1016/j.amf.2024.200134

87. Wu B, Yang YH, Shi J et al (2019) A biologically inspired hierarchical PCL/F127 scaffold for esophagus tissue repair. *Mater Lett* 243:132–135. https://doi.org/10.1016/j.matlet.2019.02.011
88. He JK, Xu FY, Dong RN et al (2017) Electrohydrodynamic 3D printing of microscale poly (ε-caprolactone) scaffolds with multi-walled carbon nanotubes. *Biofabrication* 9(1):015007. https://doi.org/10.1088/1758-5090/aa53bc
89. Xie CQ, Gao Q, Wang P et al (2019) Structure-induced cell growth by 3D printing of heterogeneous scaffolds with ultrafine fibers. *Mater Des* 181:108092. https://doi.org/10.1016/j.matdes.2019.108092
90. Bai L, Xu MG, Meng ZJ et al (2024) Coaxial electrohydrodynamic printing of core–shell microfibrous scaffolds with layer-specific growth factors release for enthesis regeneration. *Int J Extreme Manuf* 6(5):055003. https://doi.org/10.1088/2631-7990/ad5806
91. Rice TW, Bronner MP (2011) The esophageal wall. *Thorac Surg Clin* 21(2):299–305. https://doi.org/10.1016/j.thorsurg.2011.01.005
92. Squier CA, Kremer MJ (2001) Biology of oral mucosa and esophagus. *J Natl Cancer Inst Monogr* 2001(29):7–15. https://doi.org/10.1093/oxfordjournals.jncimonographs.a003443
93. Creff J, Courson R, Mangeat T et al (2019) Fabrication of 3D scaffolds reproducing intestinal epithelium topography by high-resolution 3D stereolithography. *Biomaterials* 221:119404. https://doi.org/10.1016/j.biomaterials.2019.119404
94. Zheng SY, Lavrenyuk K, Lamson NG et al (2020) Piperazine derivatives enhance epithelial cell monolayer permeability by increased cell force generation and loss of cadherin structures. *ACS Biomater Sci Eng* 6(1):367–374. https://doi.org/10.1021/acsbiomaterials.9b01660
95. Eswarakumar VP, Lax I, Schlessinger J (2005) Cellular signaling by fibroblast growth factor receptors. *Cytokine Growth Factor Rev* 16(2):139–149. https://doi.org/10.1016/j.cytogfr.2005.01.001
96. Kim HN, Hong Y, Kim MS et al (2012) Effect of orientation and density of nanotopography in dermal wound healing. *Biomaterials* 33(34):8782–8792. https://doi.org/10.1016/j.biomaterials.2012.08.038
97. Watson CJ, Collier P, Tea I et al (2014) Hypoxia-induced epigenetic modifications are associated with cardiac tissue fibrosis and the development of a myofibroblast-like phenotype. *Hum Mol Genet* 23(8):2176–2188. https://doi.org/10.1093/hmg/DDT614
98. Quan TH, Wang F, Shao Y et al (2013) Enhancing structural support of the dermal microenvironment activates fibroblasts, endothelial cells, and keratinocytes in aged human skin *in vivo*. *J Investig Dermatol* 133(3):658–667. https://doi.org/10.1038/jid.2012.364
99. Tian WQ, Liu XH, Ren K et al (2023) Biomimetic Janus film fabricated via cryogenic electrospinning for gastrointestinal mucosa repair. *Mater Des* 228:111839. https://doi.org/10.1016/j.matdes.2023.111839
100. Kim IG, Wu YR, Park SA et al (2023) Assessment of esophageal reconstruction via bioreactor cultivation of a synthetic scaffold in a canine model. *Clin Exp Otorhinolaryngol* 16(2):165–176. https://doi.org/10.21053/ceo.2022.01522
101. Shi J, Yang Y, Cheng A et al (2020) Metabolism of vascular smooth muscle cells in vascular diseases. *Am J Physiol Heart Circ Physiol* 319(3):H613–H631. https://doi.org/10.1152/ajpheart.00220.2020
102. Wang NX, Zheng WF, Cheng SY et al (2017) In vitro evaluation of essential mechanical properties and cell behaviors of a novel polylactic-co-glycolic acid (PLGA)-based tubular scaffold for small-diameter vascular tissue engineering. *Polymers* 9(8):318. https://doi.org/10.3390/polym9080318
103. Duan NN, Geng X, Ye L et al (2016) A vascular tissue engineering scaffold with core-shell structured nano-fibers formed by coaxial electrospinning and its biocompatibility evaluation. *Biomed Mater* 11(3):035007. https://doi.org/10.1088/1748-6041/11/3/035007
104. Gao G, Kim H, Kim BS et al (2019) Tissue-engineering of vascular grafts containing endothelium and smooth-muscle using triple-coaxial cell printing. *Appl Phys Rev* 6(4):041402. https://doi.org/10.1063/1.5099306